

# Concurrent Spacecraft Attitude and Orbit Estimation with Attitude Control Based on Magnetometer, Gyro, and GPS Measurements through Extended Kalman Filter

Tamer Mekky Ahmed Habib\*

*The Egyptian National Authority for Remote Sensing and Space Science, Cairo, Egypt*

**Abstract:** The main objective of this research is to provide attitude estimation, orbit estimation, and attitude control algorithms suitable for application to the next Egyptian scientific satellite. Concurrent spacecraft orbit and attitude estimates must be suitable for usage by the attitude control algorithm. The developed estimation algorithms are able to deal with severe tumbling conditions characterized by large initial attitude, angular velocity and position estimation errors. The estimation algorithms could provide attitude estimates within  $0.5^\circ(3-\sigma)$  and 60 m ( $3-\sigma$ ) for the position estimation errors. The attitude control algorithm developed is able to bring the spacecraft from its initial tumbling conditions to nadir pointing within an error of only  $0.5^\circ(3-\sigma)$ .

**Keywords:** Attitude, Orbit, Control, Estimation, EKF, GPS, Gyro, Magnetometer.

## 1. INTRODUCTION

When the satellite leaves its launching vehicle it enters an operation mode called the detumbling mode. The detumbling mode is characterized by high angular velocities and large satellite attitude angles. The task of the attitude and orbit control system (AOCS) of an earth pointing satellite is to slow down this angular motion and bring the satellite to nadir pointing. To do so, the AOCS must implement suitable algorithms for attitude and orbit estimation with attitude control. These estimation algorithms should provide attitude and orbit estimates to the attitude control algorithm. Both estimation and control algorithms must be able to deal with large initial attitude angles and angular rates [1] provided algorithms for spacecraft attitude estimation based on magnetometer measurements. But the results obtained were valid only for small attitude angles [2] describes the process of magnetic attitude estimation of a tumbling spacecraft. The process didn't include solutions neither to the problems of the attitude control nor orbit estimation [3] deals with the problem of attitude and orbit determination and control for a small geostationary satellite. Orbit estimation process isn't included in this study. In [4], the problem of spacecraft attitude and orbit estimation with attitude control is addressed but the estimation process was basically dominated by magnetometer measurements. The process of attitude estimation based on magnetometer measurements usually is characterized by slow convergence [5], described the process of fast spacecraft orbit and attitude estimation, but it didn't

include the process of attitude control [6] discussed the process of spacecraft attitude estimation and control. But due to the absence of orbit estimation process, the attitude angles converged slowly (typically after 3 orbits) [7] also didn't include the process of orbit estimation. In addition, the algorithms discussed were limited to coarse (not fine) attitude estimates (typically within  $6^\circ$ ) [8] discussed the problem of attitude estimation but the resulting attitude estimates hadn't been feedback to the control algorithm. Furthermore, the problem of orbit estimation isn't discussed at all.

The main objective of this research is to provide high accuracy attitude estimation, orbit estimation, and attitude control algorithms suitable for application to the next Egyptian scientific satellite during the detumbling and attitude acquisition modes. The estimation algorithms provided high accuracy estimates (typically within  $0.5^\circ 3-\sigma$  for attitude estimates and 60 m  $3-\sigma$  for the orbital estimates). To do so, the work done in [4, 5] is extended to provide high accuracy fast converging attitude and orbit estimates needed by the attitude control algorithm. The provided algorithms are capable of dealing with high angular velocities and large attitude errors usually characterizing the detumbling and attitude acquisition modes. The attitude control algorithm presented is capable of bringing the satellite from the detumbling mode to the attitude acquisition mode within an error of only  $0.5^\circ(3-\sigma)$ . The measurement sensors utilized were, GPS receiver, magnetometer, and gyro. GPS, and magnetometer, measurements are used to provide estimates of the spacecraft orbital motion while as magnetometer and gyro measurements are used to provide estimates of spacecraft attitude.

\*Address correspondence to these authors at the 23 Joseph Broz Teto St., El Nozha El Gedida, Cairo, Egypt; Tel: +201117154301; E-mail: tamermekky@hotmail.com

## 2. MODELING SPACECRAFT ATTITUDE AND ORBITAL MOTION

The first step to model the spacecraft orbital and attitude motion is to select the elements of the state vector. The state vector is selected to be

$$X = \begin{bmatrix} X_I & Y_I & Z_I & \dot{X}_I & \dot{Y}_I & \dot{Z}_I & q_1 & q_2 & q_3 & q_4 & \omega_x & \omega_y & \omega_z \end{bmatrix}^T \quad (1)$$

Where

$\begin{bmatrix} X_I & Y_I & Z_I \end{bmatrix}$ : Are the components of the spacecraft position vector defined in the Earth Centered Inertial Coordinate System.

$\begin{bmatrix} \dot{X}_I & \dot{Y}_I & \dot{Z}_I \end{bmatrix}$ : Are the components of the spacecraft velocity vector defined in the Earth Centered Inertial Coordinate System.

$\begin{bmatrix} q_1 & q_2 & q_3 & q_4 \end{bmatrix}$ : Are the quaternion vector representing the rotation from Earth Centered Inertial Coordinate System to the Body Coordinate System.

$\begin{bmatrix} \omega_x & \omega_y & \omega_z \end{bmatrix}$ : Are the components of the spacecraft Inertial angular velocity.

The orbital and attitude dynamics now could be written as [4, 5].

$$\dot{X} = \begin{bmatrix} \dot{X}_O \\ \dot{X}_A \end{bmatrix} = \begin{bmatrix} f_{11} & f_{12} \\ f_{21} & f_{22} \end{bmatrix} \begin{bmatrix} X_O \\ X_A \end{bmatrix} + \begin{bmatrix} B_O \\ B_A \end{bmatrix} + \eta = f(X) + B + \eta \quad (2)$$

$$f_{11} = \begin{bmatrix} 0_{3 \times 3} & I_{3 \times 3} \\ \frac{-\mu_E}{\|R\|^3} I_{3 \times 3} & 0_{3 \times 3} \end{bmatrix}, \quad f_{12} = 0_{6 \times 7}, \quad f_{21} = 0_{7 \times 6},$$

$$f_{22} = \begin{bmatrix} \frac{1}{2} \Omega & 0_{4 \times 3} \\ 0_{3 \times 4} & J^{-1} [(J\omega + H_w) \times] \end{bmatrix}, \quad B_O = \begin{bmatrix} 0_{3 \times 1} \\ a_I \end{bmatrix}, \quad \text{and}$$

$$B_A = \begin{bmatrix} 0_{4 \times 1} \\ J^{-1} T \end{bmatrix}$$

Where

$0_{i \times j}$ : Is an  $i \times j$  zero matrix.

$I_{i \times j}$ : Is an  $i \times j$  unit matrix.

$\mu_E$ : Is the earth's gravitational constant ( $\mu_E = 3.986 \times 10^{14} \text{ m}^3 / \text{s}^2$ ).

$\Omega$ : Is the skew symmetric matrix defined by

$$\Omega = \begin{bmatrix} 0 & \omega_z & -\omega_y & \omega_x \\ -\omega_z & 0 & \omega_x & \omega_y \\ \omega_y & -\omega_x & 0 & \omega_z \\ -\omega_x & -\omega_y & -\omega_z & 0 \end{bmatrix}$$

$J$ : Is the spacecraft inertia tensor given as

$$J = \begin{bmatrix} J_{xx} & -J_{xy} & -J_{xz} \\ -J_{yx} & J_{yy} & -J_{yz} \\ -J_{zx} & -J_{zy} & J_{zz} \end{bmatrix}.$$

$H_w$ : Is the angular momentum of the wheels.

$[\beta \times]$ : Is the cross product matrix of

$[\beta] = [\beta_x \ \beta_y \ \beta_z]^T$  calculated from

$$[\beta \times] = \begin{bmatrix} 0 & -\beta_z & \beta_y \\ \beta_z & 0 & -\beta_x \\ -\beta_y & \beta_x & 0 \end{bmatrix}$$

$a_I$ : Is the inertial acceleration.

$T$ : Is the Torque acting on the Spacecraft

$$X_O = \begin{bmatrix} X_I & Y_I & Z_I & \dot{X}_I & \dot{Y}_I & \dot{Z}_I \end{bmatrix}^T \quad \text{and}$$

$$X_A = \begin{bmatrix} q_1 & q_2 & q_3 & q_4 & \omega_x & \omega_y & \omega_z \end{bmatrix}^T$$

$\eta$ : Is a zero mean Gaussian white-noise.

## 3. SPACECRAFT ATTITUDE CONTROL

There exists a quaternion error vector which expresses the rotation from the spacecraft attitude direction in space,  $q^{R \rightarrow B}$ , and the target attitude direction toward which the satellite is oriented at the end of the attitude maneuver,  $q_T$  [9]. The spacecraft attitude direction in space is parameterized by the attitude quaternion representing the rotation from the reference coordinate system to the body coordinate system,  $q^{R \rightarrow B}$ . The reference coordinate system has its

x axis pointing in the direction of the spacecraft velocity in its orbit, its z direction is nadir direction, and its y direction completes a right hand rule orthogonal coordinate system. The quaternion error vector is given by [9, 10].

$$q_E = \begin{bmatrix} q_{1E} \\ q_{2E} \\ q_{3E} \\ q_{4E} \end{bmatrix} = \begin{bmatrix} q_{T4} & q_{T3} & -q_{T2} & q_{T1} \\ -q_{T3} & q_{T4} & q_{T1} & q_{T2} \\ q_{T2} & -q_{T1} & q_{T4} & q_{T3} \\ -q_{T1} & -q_{T2} & -q_{T3} & q_{T4} \end{bmatrix} \begin{bmatrix} -q_1^{R \rightarrow B} \\ -q_2^{R \rightarrow B} \\ -q_3^{R \rightarrow B} \\ q_4^{R \rightarrow B} \end{bmatrix} \quad (3)$$

The nonlinear control law is given by

$$T_{cxr} = 2K_x q_{1E} q_{4E} + K_{xd} \omega_{BRx} \quad (4)$$

$$T_{cyr} = 2K_y q_{2E} q_{4E} + K_{yd} \omega_{BRy} \quad (5)$$

$$T_{czr} = 2K_z q_{3E} q_{4E} + K_{zd} \omega_{BRz} \quad (6)$$

Where

$T_{cxr}$ ,  $T_{cyr}$ , and  $T_{czr}$ : Are control torques in the directions of the body axes triad system.

$K_x$ ,  $K_{xd}$ ,  $K_y$ ,  $K_{yd}$ ,  $K_z$ , and  $K_{zd}$ : Are the controller gains.

$\omega_{BRx}$ ,  $\omega_{BRy}$ , and  $\omega_{BRz}$ : Are the angular velocities of the body frame with respect to the reference frame.

Note that the quaternion vector,  $q^{R \rightarrow B}$ , is to be provided by the estimation algorithm.

#### 4. EXTENDED KALMAN FILTER

GPS and magnetometer provide strong observability of the spacecraft orbital states because GPS could measure directly the spacecraft position vector and the magnetometer measurements are also functions of spacecraft position. Information of spacecraft attitude is considered to be sufficient when the attitude sensors could measures two or more vectors in the spacecraft body frame of reference. Thus, magnetometer and gyro measurements are used to provide these two vectors (which are namely: the earth's magnetic field vector, and the angular velocity vector) required by the attitude estimation algorithm to solve the attitude problem unambiguously. Therefore, magnetometer and gyro measurements assure full observability of the spacecraft attitude states. In addition, magnetometers and gyros are utilized as sensors because:

1. They are commonly used devices onboard most spacecraft orbiting the earth.
2. Their ability to work during spacecraft detumbling, attitude acquisition, standby, and high accuracy modes. And the problem at hand requires sensors such as magnetometer and gyro those are able to operate at these conditions.
3. Commonly used attitude sensors could not be used at the problem at hand. For example, the sun sensor provides intermittent information only due to shadow over the sensor. The star sensor also could not be used because the spacecraft is detumbling, and using of such sensor requires high accuracy modes only.

Finally, this set of sensors could sufficiently provide full observability of the spacecraft orbital and attitude states so as to provide high rate of convergence. The same structure of the extended Kalman filter found in [5] is utilized. The only difference exists in the measurement vector and its corresponding measurement matrix. The measurement vector is given by

$$h = \begin{bmatrix} b_{xb} & b_{yb} & b_{zb} & \omega_x & \omega_y & \omega_z & X_I & Y_I & Z_I \end{bmatrix} + v \quad (7)$$

Where  $v$  is a zero mean Gaussian white noise. And the corresponding measurement matrix is given by

$$\frac{\partial h}{\partial X} = \begin{bmatrix} \frac{\partial b_{xb}}{\partial X_I} & \frac{\partial b_{xb}}{\partial Y_I} & \frac{\partial b_{xb}}{\partial Z_I} & \frac{\partial b_{xb}}{\partial X_I} & \frac{\partial b_{xb}}{\partial Y_I} & \frac{\partial b_{xb}}{\partial Z_I} & \frac{\partial b_{xb}}{\partial q_1} & \frac{\partial b_{xb}}{\partial q_2} & \frac{\partial b_{xb}}{\partial q_3} & \frac{\partial b_{xb}}{\partial q_4} & \frac{\partial b_{xb}}{\partial \omega_x} & \frac{\partial b_{xb}}{\partial \omega_y} & \frac{\partial b_{xb}}{\partial \omega_z} \\ \frac{\partial b_{yb}}{\partial X_I} & \frac{\partial b_{yb}}{\partial Y_I} & \frac{\partial b_{yb}}{\partial Z_I} & \frac{\partial b_{yb}}{\partial X_I} & \frac{\partial b_{yb}}{\partial Y_I} & \frac{\partial b_{yb}}{\partial Z_I} & \frac{\partial b_{yb}}{\partial q_1} & \frac{\partial b_{yb}}{\partial q_2} & \frac{\partial b_{yb}}{\partial q_3} & \frac{\partial b_{yb}}{\partial q_4} & \frac{\partial b_{yb}}{\partial \omega_x} & \frac{\partial b_{yb}}{\partial \omega_y} & \frac{\partial b_{yb}}{\partial \omega_z} \\ \frac{\partial b_{zb}}{\partial X_I} & \frac{\partial b_{zb}}{\partial Y_I} & \frac{\partial b_{zb}}{\partial Z_I} & \frac{\partial b_{zb}}{\partial X_I} & \frac{\partial b_{zb}}{\partial Y_I} & \frac{\partial b_{zb}}{\partial Z_I} & \frac{\partial b_{zb}}{\partial q_1} & \frac{\partial b_{zb}}{\partial q_2} & \frac{\partial b_{zb}}{\partial q_3} & \frac{\partial b_{zb}}{\partial q_4} & \frac{\partial b_{zb}}{\partial \omega_x} & \frac{\partial b_{zb}}{\partial \omega_y} & \frac{\partial b_{zb}}{\partial \omega_z} \\ 0 & 0 & 0 & 0 & 0 & 0 & 0 & 0 & 0 & 0 & 1 & 0 & 0 \\ 0 & 0 & 0 & 0 & 0 & 0 & 0 & 0 & 0 & 0 & 0 & 1 & 0 \\ 0 & 0 & 0 & 0 & 0 & 0 & 0 & 0 & 0 & 0 & 0 & 0 & 1 \\ 1 & 0 & 0 & 0 & 0 & 0 & 0 & 0 & 0 & 0 & 0 & 0 & 0 \\ 0 & 1 & 0 & 0 & 0 & 0 & 0 & 0 & 0 & 0 & 0 & 0 & 0 \\ 0 & 0 & 1 & 0 & 0 & 0 & 0 & 0 & 0 & 0 & 0 & 0 & 0 \end{bmatrix} \quad (8)$$

Details of computing the measurement matrix are given in [4] by

$$\frac{\partial b_{xb}}{\partial X_I} = A_{11} \frac{\partial b_{xI}}{\partial X_I} + A_{12} \frac{\partial b_{yI}}{\partial X_I} + A_{13} \frac{\partial b_{zI}}{\partial X_I} \quad (9)$$

$$\frac{\partial b_{xb}}{\partial Y_I} = A_{11} \frac{\partial b_{xI}}{\partial Y_I} + A_{12} \frac{\partial b_{yI}}{\partial Y_I} + A_{13} \frac{\partial b_{zI}}{\partial Y_I} \quad (10)$$

$$\frac{\partial b_{xb}}{\partial Z_I} = A_{11} \frac{\partial b_{xI}}{\partial Z_I} + A_{12} \frac{\partial b_{yI}}{\partial Z_I} + A_{13} \frac{\partial b_{zI}}{\partial Z_I} \quad (11)$$

$$\frac{\partial b_{yb}}{\partial X_l} = A_{21} \frac{\partial b_{xl}}{\partial X_l} + A_{22} \frac{\partial b_{yl}}{\partial X_l} + A_{23} \frac{\partial b_{zl}}{\partial X_l} \tag{12}$$

$$\frac{\partial b_{yb}}{\partial Y_l} = A_{21} \frac{\partial b_{xl}}{\partial Y_l} + A_{22} \frac{\partial b_{yl}}{\partial Y_l} + A_{23} \frac{\partial b_{zl}}{\partial Y_l} \tag{13}$$

$$\frac{\partial b_{yb}}{\partial Z_l} = A_{21} \frac{\partial b_{xl}}{\partial Z_l} + A_{22} \frac{\partial b_{yl}}{\partial Z_l} + A_{23} \frac{\partial b_{zl}}{\partial Z_l} \tag{14}$$

$$\frac{\partial b_{zb}}{\partial X_l} = A_{31} \frac{\partial b_{xl}}{\partial X_l} + A_{32} \frac{\partial b_{yl}}{\partial X_l} + A_{33} \frac{\partial b_{zl}}{\partial X_l} \tag{15}$$

$$\frac{\partial b_{zb}}{\partial Y_l} = A_{31} \frac{\partial b_{xl}}{\partial Y_l} + A_{32} \frac{\partial b_{yl}}{\partial Y_l} + A_{33} \frac{\partial b_{zl}}{\partial Y_l} \tag{16}$$

$$\frac{\partial b_{zb}}{\partial Z_l} = A_{31} \frac{\partial b_{xl}}{\partial Z_l} + A_{32} \frac{\partial b_{yl}}{\partial Z_l} + A_{33} \frac{\partial b_{zl}}{\partial Z_l} \tag{17}$$

Where  $b_{xl}$  is the inertial component of the earth's magnetic field vector, and

$$\begin{bmatrix} A_{11} & A_{12} & A_{13} \\ A_{21} & A_{22} & A_{23} \\ A_{31} & A_{32} & A_{33} \end{bmatrix} = \begin{bmatrix} q_1^2 - q_2^2 - q_3^2 + q_4^2 & 2(q_1q_2 + q_3q_4) & 2(q_1q_3 - q_2q_4) \\ 2(q_1q_2 - q_3q_4) & -q_1^2 + q_2^2 - q_3^2 + q_4^2 & 2(q_2q_3 + q_1q_4) \\ 2(q_1q_3 + q_2q_4) & 2(q_2q_3 - q_1q_4) & -q_1^2 - q_2^2 + q_3^2 + q_4^2 \end{bmatrix} \tag{18}$$

Also we have

$$\frac{\partial b_{xb}}{\partial q_1} = 2q_1b_{xl} + 2q_2b_{yl} + 2q_3b_{zl} \tag{19}$$

$$\frac{\partial b_{xb}}{\partial q_2} = -2q_2b_{xl} + 2q_1b_{yl} - 2q_4b_{zl} \tag{20}$$

$$\frac{\partial b_{xb}}{\partial q_3} = -2q_3b_{xl} + 2q_4b_{yl} + 2q_1b_{zl} \tag{21}$$

$$\frac{\partial b_{xb}}{\partial q_4} = 2q_4b_{xl} + 2q_3b_{yl} - 2q_2b_{zl} \tag{22}$$

$$\frac{\partial b_{yb}}{\partial q_1} = 2q_2b_{xl} - 2q_1b_{yl} + 2q_4b_{zl} \tag{23}$$

$$\frac{\partial b_{yb}}{\partial q_2} = 2q_1b_{xl} + 2q_2b_{yl} + 2q_3b_{zl} \tag{24}$$

$$\frac{\partial b_{yb}}{\partial q_3} = -2q_4b_{xl} - 2q_3b_{yl} + 2q_2b_{zl} \tag{25}$$

$$\frac{\partial b_{yb}}{\partial q_4} = -2q_3b_{xl} + 2q_4b_{yl} + 2q_1b_{zl} \tag{26}$$

$$\frac{\partial b_{zb}}{\partial q_1} = 2q_3b_{xl} - 2q_4b_{yl} - 2q_1b_{zl} \tag{27}$$

$$\frac{\partial b_{zb}}{\partial q_2} = 2q_4b_{xl} + 2q_3b_{yl} - 2q_2b_{zl} \tag{28}$$

$$\frac{\partial b_{zb}}{\partial q_3} = 2q_1b_{xl} + 2q_2b_{yl} + 2q_3b_{zl} \tag{29}$$

$$\frac{\partial b_{zb}}{\partial q_4} = 2q_2b_{xl} - 2q_1b_{yl} + 2q_4b_{zl} \tag{30}$$

### 5. OBSERVABILITY AND CONTROLLABILITY ANALYSIS

Check of the observability and controllability matrices could be done through the computation of the observability and controllability matrices. The observability matrix,  $OB$ , is given by

$$OB = \begin{bmatrix} H_k \\ H_k A_k \\ H_k A_k^2 \\ \vdots \\ H_k A_k^{12} \end{bmatrix} \tag{31}$$

And the controllability matrix is given by

$$CO = \begin{bmatrix} G & A_k G & A_k^2 G & \dots & A_k^{12} G \end{bmatrix} \tag{32}$$

Where the matrix,  $G$ , is given by

$$G = \begin{bmatrix} 0_{3 \times 3} & 0_{3 \times 3} \\ I_{3 \times 3} & 0_{3 \times 3} \\ 0_{4 \times 3} & 0_{4 \times 3} \\ 0_{3 \times 3} & J^{-1} \end{bmatrix} \tag{33}$$

Thus, for complete controllability and observability the controllability and observability matrices must have a full rank.

### 6. BLOCK DIAGRAMS AND FLOW CHARTS

To clarify the relation between the estimation and control algorithms, a block diagram is given below in Figure 1.

To summarize the solution procedure, A flow chart is given in Figure 2.

### 7. A SIMULATION CASE STUDY

In order to verify the developed methodologies, a case study spacecraft is utilized. The spacecraft initial conditions are:  $a$  (semi major axis) = 7189200 m,  $e$  (orbit eccentricity) = 0.01,  $i$  (orbit inclination) = 100.585°,  $\Omega$  (right ascension of ascending node) = 339.5°,  $\vartheta$  (argument of perigee) = 69°, and  $v$  (true

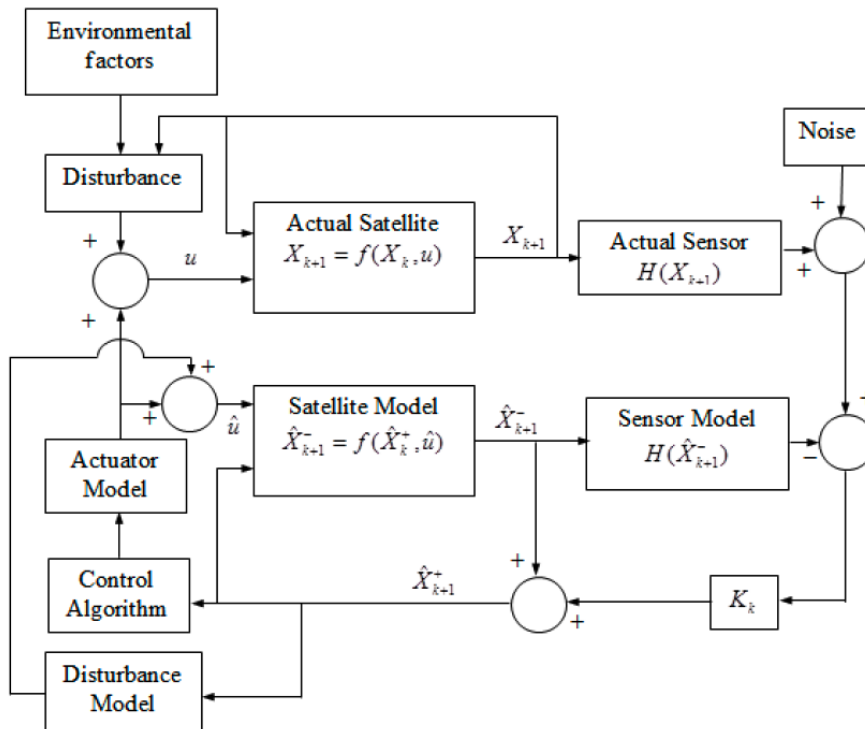


Figure 1: Relationship between control and estimation algorithms.

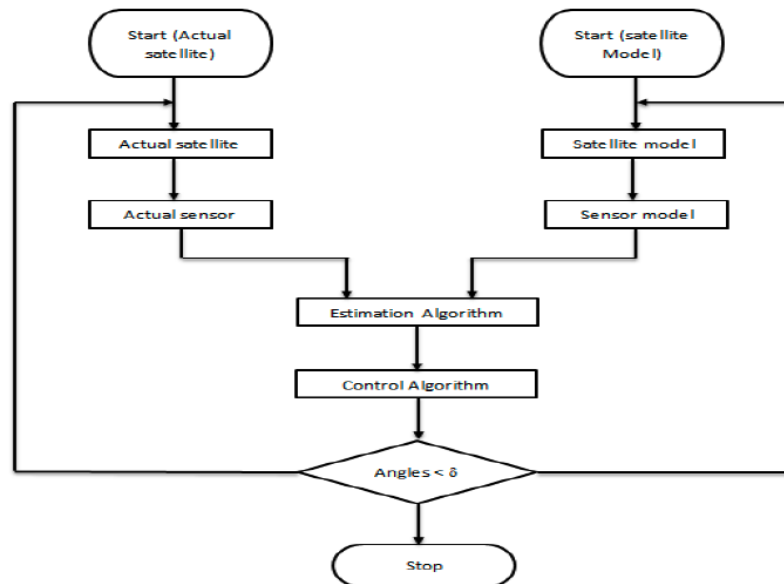
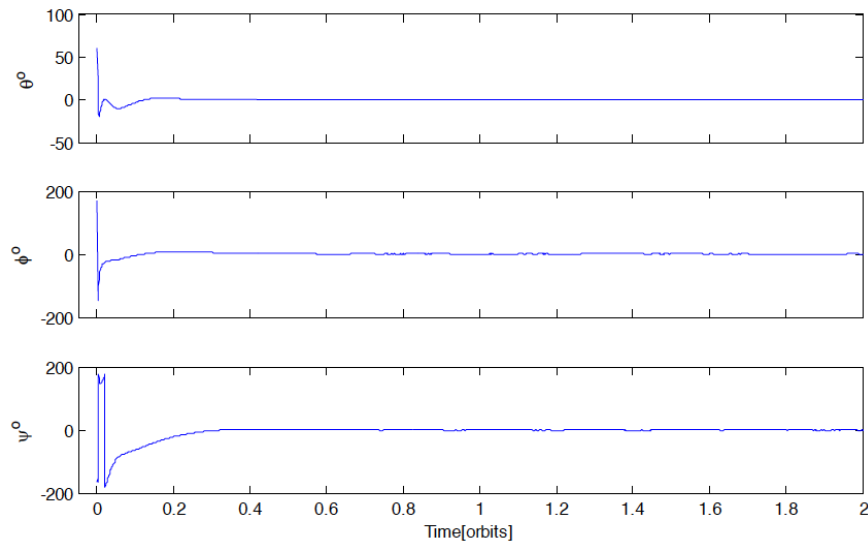


Figure 2: Flow chart of estimation and control algorithms.

anomaly) =  $3.5^\circ$ .  $\phi$  (roll angle) =  $170^\circ$ ,  $\psi$  (yaw angle) =  $-165^\circ$ , and  $\theta$  (pitch angle) =  $60^\circ$ . The inertial angular velocity components are  $\omega_x = 4^\circ/\text{sec}$ ,  $\omega_y = 4^\circ/\text{sec}$ , and  $\omega_z = -2^\circ/\text{sec}$ .

The estimator initial conditions are:  $a$  (semi major axis) = 7039200 m,  $e$  (orbit eccentricity) = 0,  $i$  (orbit inclination) =  $98.085^\circ$ ,  $\Omega$  (right ascension of ascending

node) =  $337.5^\circ$ ,  $\vartheta$  (argument of perigee) =  $69^\circ$ , and  $v$  (true anomaly) =  $0^\circ$ .  $\phi$  (roll angle) =  $0^\circ$ ,  $\psi$  (yaw angle) =  $0^\circ$ , and  $\theta$  (pitch angle) =  $0^\circ$ . The inertial angular velocity components are  $\omega_x = 0^\circ/\text{sec}$ ,  $\omega_y = -0.0011^\circ/\text{sec}$ , and  $\omega_z = 0^\circ/\text{sec}$ . Figure 3. Represents the time history of the spacecraft attitude angles. As seen in this figure, the initial attitude angles were as large 170 degree. The control algorithm discussed is



**Figure 3:** Spacecraft attitude time history.

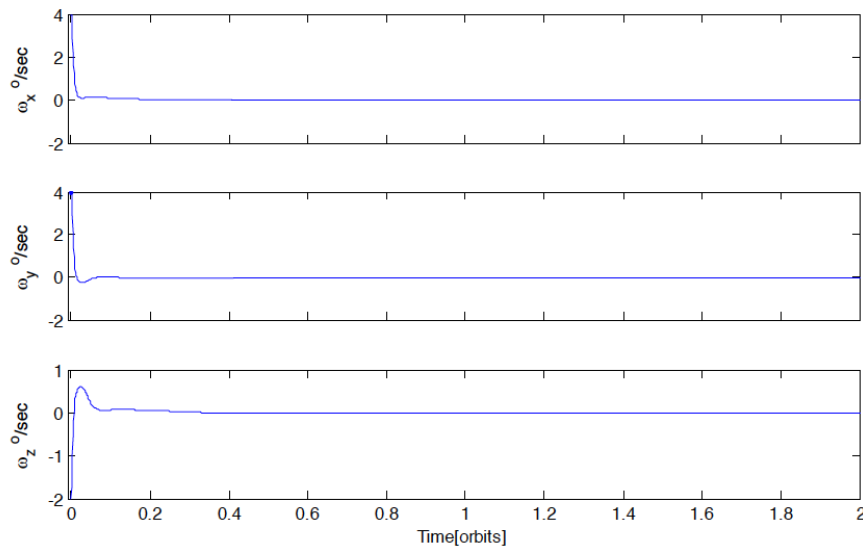


**Figure 4:** Spacecraft inertial angular velocity time history.

capable of dealing with these large angles which are encountered during the detumbling mode. Figure 4 shows the time history of the spacecraft inertial angular velocities. As clear in Figures 3 and 4, the attitude control algorithm succeeded in bringing the satellite from the detumbling mode to nadir pointing in less than half of an orbit. Controller gains are chosen in accordance with [11]. The controller gains are  $\begin{bmatrix} 5.52 \times 10^{-3} & 0.484 & 5.62 \times 10^{-3} & 0.49 & 4.54 \times 10^{-3} & 0.4 \end{bmatrix}$  respectively. These gains could be adjusted off line to achieve higher performance using any optimization technique such as genetic algorithms, particle swarm optimization, ant colony optimization, or simulated annealing.

Figure 5 displays the time history of the spacecraft attitude estimation error of the pitch, roll, and yaw

angles respectively. The maximum estimation error was about  $0.5^o$  ( $3-\sigma$ ). Figure 6 represents the time history of the magnitude of the position estimation error. The initial magnitude of the position estimation error was about 452 Km. After only one time step this error has been reduced drastically to 60 m ( $3-\sigma$ ). This drastic reduction is basically achieved due to the existence of GPS measurements which increase the observability of the spacecraft position and velocity vectors. Note that also equation (7) states that spacecraft position vector is measured directly through the GPS receiver. As computed, the rank of the observability and controllability matrices is always equal to 13, which indicates full observability and controllability of the system states.

Table 1 shows a comparison between the current research results and the results of reference [5]

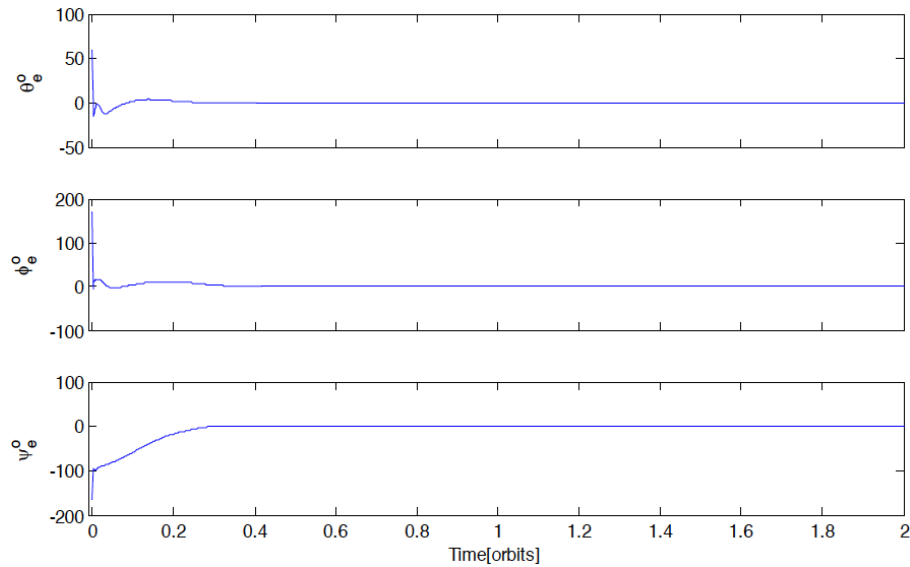


Figure 5: Spacecraft attitude estimation error time history.

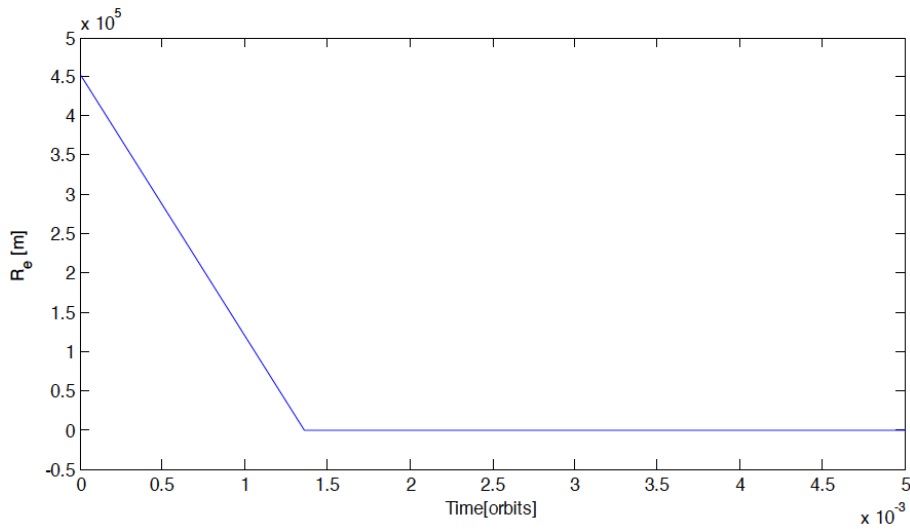


Figure 6: Position estimation error time history.

Table 1: A Comparison between the Algorithms Developed in Reference [5], and Current Research Algorithm

	Algorithm developed in [5]	Current research algorithm
Sensors utilized	Star sensor, magnetometer, gyroscope, and GPS	Magnetometer, gyroscope, and GPS
Satellite operation mode	High accuracy operation mode	Detumbling, stand-by mode, and high accuracy operation modes
Attitude and orbit estimates are fed back to the attitude control algorithm	No, because there is no attitude control algorithm.	Yes

8. CONCLUSION

The methods of spacecraft orbit and attitude estimation during the detumbling and attitude acquisition modes had worked effectively with each

other despite of large initial attitude and orbit estimation errors. The estimation error was about  $0.5^\circ$  ( $3-\sigma$ ) for the attitude angles and 60 m ( $3-\sigma$ ) for the position estimation error. Both estimates of spacecraft attitude and orbit are fed successfully to the attitude control

algorithm. The attitude control algorithm was able to bring the satellite from the detumbling mode to nadir pointing during less than half of an orbit within accuracy of  $0.5^\circ$  ( $3-\sigma$ ). The rank of the observability and controllability matrices was thirteen, which is indicating a full rank, so the plant is considered to be fully observable and controllable.

## 9. FUTURE STUDY

Note that, it is assumed that the only source of errors is zero mean Gaussian white noise as clarified by equations (2), and (7). There are also several sources of errors which could affect the overall suggested algorithm performance, and robustness. These sources could be due to one of the following reasons:

- 1- Sensor bias offset.
- 2- Sensor bias drift rate.
- 3- Sensor colored noise.
- 4- Scale factor stability and dependence on the operating temperature.
- 5- Sensor, and actuator dynamics.
- 6- Axes non-orthogonality
- 7- Sensor and actuator mounting errors.

Also various methods of control and control gain optimization could be utilized to optimize the controller performance according to a prescribed cost function identified by the control system designer. Consequently, a trade off study is important to be established among all of these alternatives. Thus, for a

complete solution of these problems a multi-disciplinary team work should be formed to study and model the effects of these highly complicated factors over the algorithm performance.

## REFERENCES

- [1] Thomas B. Spacecraft Attitude Determination- a Magnetometer Approach. PhD Thesis, Aalborg University 1999.
- [2] Erick JS. Magnetic Attitude Estimation of a Tumbling Spacecraft. MSc Thesis, California Polytechnic State University 2005.
- [3] Thopil GA. An Attitude and Orbit Determination and Control System for a Small Geostationary Satellite. MSc Thesis, Stellenbosch 2006.
- [4] Tamer M. New Algorithms of Nonlinear Spacecraft Attitude Control *via* Attitude, Angular velocity, and Orbit Estimation Based on the Earth's Magnetic Field. PhD Thesis, Cairo University 2009.
- [5] Tamer M. Fast Converging with High Accuracy Estimates of Satellite Attitude and Orbit Based on Magnetometer Augmented with Gyro, Star Sensor and GPS *via* Extended Kalman Filter. EJRS 2011; 14(2): 61-57.
- [6] Mohammad A, Sang-Young P. Integrated attitude determination and control system *via* magnetic measurements and actuation. Act Ast 2011; 69: 185-168.
- [7] Tian X, Tao M, Hao W, Ke H, Zhong J. Design and on-orbit performance of the attitude determination and control system for the eZDPS-1A pico-satellite. Act Astr 2012; 77: 196-182.
- [8] Xiaojun T, Zhenbao L, Jiasheng Z. Square-root quaternion cubature Kalman filtering for spacecraft attitude estimation. Act Astr 2012; 76: 84-9. <http://dx.doi.org/10.1016/j.actaastro.2012.02.009>
- [9] Marcel JS. Spacecraft Dynamics and Control, a Practical Engineering Approach. 1<sup>st</sup> ed. Cambridge University Press; 1997.
- [10] Hinagawa H, Yamaoka H, Hanada T. Orbit determination by genetic algorithm and application to GEO observation. Adv in SpcRsrch 2014; 53: 542-532.
- [11] Tamer M. The Global Positioning System Application to Satellite Position and Attitude Determination. MSc thesis, Aerospace Department, Cairo University 2003.

Received on 04-09-2014

Accepted on 01-10-2014

Published on 22-10-2014

<http://dx.doi.org/10.6000/1927-5129.2014.10.61>

© 2014 Tamer Mekky Ahmed Habib; Licensee Lifescience Global.

This is an open access article licensed under the terms of the Creative Commons Attribution Non-Commercial License (<http://creativecommons.org/licenses/by-nc/3.0/>) which permits unrestricted, non-commercial use, distribution and reproduction in any medium, provided the work is properly cited.